Int. J. Multiphase Flow Vol. 16, No. 2, pp. 341–351, 1990
Printed in Great Britain.

0301-9322/90 $3.00 + 0.00

A THERMODYNAMICAL FORMULATION FOR DISPERSED MULTIPHASE TURBULENT FLOWS—II

SIMPLE SHEAR FLOWS FOR DENSE MIXTURES

D. MA and G. AHMADI
Department of Mechanical & Industrial Engineering, Clarkson University, Potsdam, NY 13676, U.S.A.

(*Received* 7 *July* 1987; *in revised form* 1 *October* 1989)

Abstract—Using the turbulence model for dispersed multiphase flows developed in Part I [*Int. J. Multiphase Flow* **16**, 323–340 (1990)], simple shear flows of a dense solid–fluid mixture are studied. The equations governing the transport of mass, momentum and fluctuation kinetic energy for different phases are reviewed and their simplified forms for the case of a simple shear flow are considered. The resulting algebraic equations for the fluctuation kinetic energies are solved by an iterative method and the variations of the normal and shear stresses with the shear rate and solid volume fraction are studied. Particular attention is given to the effects of the fluid phase. It is shown that the predictions of the model agree reasonably well with the available experimental data.

Key Words: turbulent flow, multiphase mixture, simple shear, granular flow

INTRODUCTION

Understanding the dynamic behavior of turbulent multiphase flows has attracted considerable attention in recent years. Several models for dispersed two-phase turbulent flows were developed by Baw & Peskin (1971), Hetsroni & Sokolov (1972), Taweel & Landau (1977), Genchev & Karpuzov (1980), Elghobashi & Abou-Arab (1983) and Chen & Wood (1985). Extensive reviews of the literature on earlier works were provided by Soo (1967), Hetsroni (1982) and Ishii & Mishima (1984). These models were developed for relatively dilute mixtures and the particle–particle collisional effects and the fluctuation energy interactions between the fluid and particulate phases were, generally, neglected. Recently, Ma & Ahmadi (1985, 1986) developed a turbulence model for rapid flows of dense granular materials. Lun *et al.* (1984), Jenkins & Richman (1985, 1986), Ahmadi & Shahinpoor (1983) and Ahmadi & Ma (1986) formulated several elaborated kinetic theories for rapid flows of dense collections of idealized spherical granular particles. More recently, Ma & Ahmadi (1988) studied the consequences of interstitial fluid effects in the kinetic formulation.

There appear to be several deficiencies in the current state of two-phase turbulent flow and rapid granular flow modelings. The available models are either limited to dilute mixtures or neglect the fluid effects altogether. In the work of Ahmadi & Ma (1990, this issue, pp. 323–340), which will be referred to as Part I hereafter, a phasic mass-weighted averaging technique was used and a thermomechanical formulation for multiphase flows was developed. A closed system of field equations for determining the velocity, solid volume fraction and fluctuation kinetic energies of different phases was obtained. The formulation includes transport equations for the fluctuation kinetic energies of the particulate phases in addition to that of the fluid phase. Therefore, the model is suitable for analyzing turbulent flows of relatively dense mixtures.

In this work, the predictions of the turbulence model of Part I for dense flows are compared with the experimental data. In the following, the system of governing equations for a two-phase mixture is briefly reviewed. The special case of a simple shear flow of a dense mixture is carefully examined. It is shown that the governing equations reduce to a set of coupled nonlinear algebraic equations for the stresses and fluctuation energies. This system is solved by a numerical iterative scheme and the normal and shear stresses for different values of the parameters are evaluated. The variations of the normal and shear stresses with the solid volume fraction and shear rate are studied in detail and the predicted results are compared with the experimental data of Hanes & Inman (1985), Bagnold (1954) and Savage & McKeown (1983). Good agreement between the predictions of the present turbulence model and the available experimental data in the limit of rapid simple

shear flows of dense mixtures is observed. The contributions of the particulate and fluid phases to stresses and the effects of particle inelasticity are also discussed.

BASIC EQUATIONS

In Part I, the general equations governing the transport of mass, momentum and fluctuation energy for multiphase mixtures were obtained. In the special case of an isothermal, fully-saturated two-phase flow with incompressible fluid and particulate constituents, these equations are given as:

conservation of mass,

$$\frac{\partial v}{\partial t}+\frac{\partial}{\partial x_j}(v\tilde{v}_j)=0 \qquad [1]$$

and

$$\frac{\partial v^{\mathrm{f}}}{\partial t}+\frac{\partial}{\partial x_j}(v^{\mathrm{f}}\tilde{v}_j^{\mathrm{f}})=0; \qquad [2]$$

balance of linear momentum,

$$\rho v\frac{\mathrm{d}\tilde{v}_i}{\mathrm{d}t}=\rho v f_i-v\frac{\partial p^{\mathrm{f}}}{\partial x_i}-\frac{\partial}{\partial x_i}[\gamma\rho vk+\tfrac{2}{3}(\mu+\mu^{\mathrm{T}})\tilde{v}_{\mathrm{m,m}}]$$
$$+\frac{\partial}{\partial x_j}\left[(\mu+\mu^{\mathrm{T}})\left(\frac{\partial\tilde{v}_i}{\partial x_j}+\frac{\partial\tilde{v}_j}{\partial x_i}\right)\right]+D_0(\tilde{v}_i^{\mathrm{f}}-\tilde{v}_i) \qquad [3]$$

and

$$\rho^{\mathrm{f}}v^{\mathrm{f}}\frac{\mathrm{d}\tilde{v}_i^{\mathrm{f}}}{\mathrm{d}t}=\rho^{\mathrm{f}}v^{\mathrm{f}}f_i^{\mathrm{f}}-v^{\mathrm{f}}\frac{\partial p^{\mathrm{f}}}{\partial x_i}-\frac{2}{3}\frac{\partial}{\partial x_i}[\rho^{\mathrm{f}}v^{\mathrm{f}}k^{\mathrm{f}}+(\mu^{\mathrm{f}}+\mu^{\mathrm{fT}})\tilde{v}_{\mathrm{m,m}}^{\mathrm{f}}]$$
$$+\frac{\partial}{\partial x_j}\left[(\mu^{\mathrm{f}}+\mu^{\mathrm{fT}})\left(\frac{\partial\tilde{v}_i^{\mathrm{f}}}{\partial x_j}+\frac{\partial\tilde{v}_j^{\mathrm{f}}}{\partial x_i}\right)\right]+D_0(\tilde{v}_i-\tilde{v}_i^{\mathrm{f}}); \qquad [4]$$

balance of fluctuation kinetic energy,

$$\rho v\frac{\mathrm{d}k}{\mathrm{d}t}=-(\gamma\rho vk+\tfrac{2}{3}\mu^{\mathrm{T}}\tilde{v}_{m,m})\frac{\partial\tilde{v}_i}{\partial x_i}+\mu^{\mathrm{T}}\left(\frac{\partial\tilde{v}_i}{\partial x_j}+\frac{\partial\tilde{v}_j}{\partial x_i}\right)\frac{\partial\tilde{v}_i}{\partial x_j}+\frac{\partial}{\partial x_i}\left(\frac{\mu^{\mathrm{T}}}{\sigma^k}\frac{\partial k}{\partial x_i}\right)$$
$$+\frac{\mu^{\mathrm{T}}}{\sigma^{\mathrm{p}}\rho vk}\frac{\partial(vp^{\mathrm{f}})}{\partial x_i}\frac{\partial(vp^{\mathrm{f}})}{\partial x_i}-\rho v\epsilon+2D_0(ck^{\mathrm{f}}-k) \qquad [5]$$

and

$$\rho^{\mathrm{f}}v^{\mathrm{f}}\frac{\mathrm{d}k^{\mathrm{f}}}{\mathrm{d}t}=-\tfrac{2}{3}(\rho^{\mathrm{f}}v^{\mathrm{f}}k^{\mathrm{f}}+\mu^{\mathrm{fT}}\tilde{v}_{\mathrm{m,m}}^{\mathrm{f}})\frac{\partial\tilde{v}_i^{\mathrm{f}}}{\partial x_i}+\mu^{\mathrm{fT}}\left(\frac{\partial\tilde{v}_i^{\mathrm{f}}}{\partial x_j}+\frac{\partial\tilde{v}_j^{\mathrm{f}}}{\partial x_i}\right)\frac{\partial\tilde{v}_i^{\mathrm{f}}}{\partial x_j}$$
$$+\frac{\partial}{\partial x_i}\left[\left(\mu^{\mathrm{f}}+\frac{\mu^{\mathrm{fT}}}{\sigma^{\mathrm{fk}}}\right)\frac{\partial k^{\mathrm{f}}}{\partial x_i}\right]+\frac{\mu^{\mathrm{fT}}}{\sigma^{\mathrm{fp}}\rho^{\mathrm{f}}v^{\mathrm{f}}k^{\mathrm{f}}}\frac{\partial(v^{\mathrm{f}}p^{\mathrm{f}})}{\partial x_i}\frac{\partial(v^{\mathrm{f}}p^{\mathrm{f}})}{\partial x_i}-\rho^{\mathrm{f}}v^{\mathrm{f}}\epsilon^{\mathrm{f}}+2D_0(k-ck^{\mathrm{f}}); \qquad [6]$$

and

saturation condition,

$$v^{\mathrm{f}}+v=1. \qquad [7]$$

In these equations, v is the solid volume fraction, ρ is the constituent density, $\tilde{v}$ is the mass-weighted average velocity, k is the fluctuation kinetic energy per unit mass, ϵ is the dissipation rate per unit mass, f is the body force per unit mass, p^{f} is the mean pressure in the fluid phase, μ is the coefficient of viscosity, μ^{T} is the coefficient of turbulence (eddy) viscosity, σ^{k} is the turbulence Prandtl number for fluctuation energy and σ^{p} is a material parameter. The superscript f refers to the fluid phase and a symbol without a superscript represents a particulate phase quantity.

Equations [1]–[7] are 11 equations for determining the 11 unknowns $\tilde{v}_i$, $\tilde{v}_i^f$, v, v^f, k, k^f and p^f. The other parameters in these equations are related to the main 11 independent variables described in Part I. The relationships which are relevant to the present case of two-phase flows are summarized in the following.

The coefficients of turbulence viscosity for particulate and fluid phases, as obtained in Part I, are given as

$$\mu^T = C^\mu \rho v d k^{1/2}, \qquad \mu^{fT} = \frac{C^{f\mu} \rho^f v^f (k^f)^2}{\epsilon^f}, \tag{8}$$

where

$$C^\mu = 0.0853[(\chi v)^{-1} + 3.2 + 12.1824 v\chi], \qquad C^{f\mu} = 0.09. \tag{9}$$

The dissipation rates for the particulate and the fluid phases are given by

$$\epsilon = a k^{3/2}, \qquad \epsilon^f = a^f (k^f)^{3/2}, \tag{10}$$

with

$$a = \frac{3.9 v\chi (1 - r^2)}{d}, \qquad a^f = \frac{C^{fD}}{\Lambda^f}, \tag{11}$$

where $C^{fD} = 0.165$ is a constant and Λ^f is a length macroscale of fluid turbulence. Here, it is assumed that the particles are spherical and nearly elastic with a diameter d and a coefficient of restitution r. The crowding effect of particles exhibits itself through the radial distribution function χ. For spherical particles, it was found that (Ma & Ahmadi 1986; Ahmadi & Ma 1986):

$$\chi = \frac{1 + 2.5v + 4.5904(v)^2 + 4.515439(v)^3}{\left[1 - \left(\frac{v}{v_m}\right)^3\right]^{0.678021}}, \tag{12}$$

with $v_m = 0.64356$. The increase in the particulate pressure is accounted for through the coefficient γ which is given as

$$\gamma = \tfrac{2}{3}(1 + 4v\chi) + \tfrac{1}{3}(1 - r^2). \tag{13}$$

In [5] and [6], the coefficient c is related to the ratio of the particle time scale $\rho v / D_0$ to the Lagrangian time macroscale of turbulence T_L, i.e.

$$c = \frac{1}{1 + \dfrac{\rho v}{D_0 T_L}}, \qquad T_L = \frac{0.165\, k^f}{\epsilon^f}. \tag{14}$$

Here, the drag coefficient is given as

$$D_0 = \frac{18\, \mu_0^f v}{(d)^2} \frac{[1 + 0.1(\mathrm{Re_d})^{0.75}]}{\left(1 - \dfrac{v}{v_m}\right)^{2.5 v_m}}, \tag{15}$$

where the particle Reynolds number is defined as

$$\mathrm{Re_d} = \frac{\rho^f d |\tilde{v}_i^f - \tilde{v}_i|}{\mu_0^f}. \tag{16}$$

The increase in drag due to the increase in solid volume fraction and particle Reynolds number is included in [15].

In [3] and [4], the effect of lift force is neglected. The more general version of the momentum equation, described in Part I, includes the lift forces and may be used as required. For the case of the simple shear flow studied in the following section, however, the effects of lift force vanish. Additional relationships were described in Part I but are not discussed in this section since they become irrelevant to the special case of the simple shear flows studied in the following.

SIMPLE SHEAR FLOWS

In this section, simple shear flows of relatively dense two-phase mixtures in the state of turbulent (rapid) motion are considered. Comparisons of the predictions of the present model with the experimental data of Hanes & Inman (1985), Bagnold (1954) and Savage & McKeown (1983) are also presented.

Consider a steady simple shear flow with $\tilde{u}^f(y)$ and $\tilde{u}(y)$ denoting the x-components of the fluid and particle velocities, respectively. Based on the constitutive equations developed for the particle and fluid stress tensors in Part I, the total normal and shear stresses for a simple shear flow are given as

$$|\tau_{11} + p^f| = \tfrac{2}{3}\rho^f(1-\nu)k^f + \gamma\rho\nu k \qquad [17]$$

and

$$\tau_{12} = (\mu^f + \mu^{fT})\frac{d\tilde{u}^f}{dy} + (\mu + \mu^T)\frac{d\tilde{u}}{dy}. \qquad [18]$$

The stresses given by [17] and [18] include the contributions from both phases.

For a steady shear flow, in the absence of body forces, the momentum equations given by [3] and [4] become

$$-\nu\frac{\partial p^f}{\partial x} + \frac{d}{dy}\left[(\mu + \mu^T)\frac{d\tilde{u}}{dy}\right] + D_0(\tilde{u}^f - \tilde{u}) = 0 \qquad [19]$$

and

$$(1-\nu)\frac{\partial p^f}{\partial x} + \frac{d}{dy}\left[(\mu^f + \mu^{fT})\frac{d\tilde{u}^f}{dy}\right] + D_0(\tilde{u} - \tilde{u}^f) = 0. \qquad [20]$$

In the absence of a pressure gradient, [19] and [20] accept a simple shear flow solution given by

$$\tilde{u}^f = \tilde{u} = u(y), \qquad [21]$$

and

$$\frac{du}{dy} = \text{const.} \qquad [22]$$

That is, no slip between the mean particle and fluid velocities exists. (Consideration of the lift force does not alter this simple solution.)

Using [21], [18] may be restated as

$$\tau_{12} = (\mu^{fT} + \mu^T)\frac{du}{dy}. \qquad [23]$$

In a turbulent two-phase flow, the fluid viscosity μ^f is much smaller than the fluid turbulence viscosity μ^{fT} and the particle frictional rolling viscosity μ is negligible; therefore, in the derivation of [23] the viscous and frictional stresses are neglected.

Equations [17] and [23] show that the normal and shear stresses are functions of fluctuation energies k^f and k. The evolution of these fluctuation energies is governed by [5] and [6]. For a steady simple shear flow, the diffusion and convection are absent and [5] and [6] simplify to

$$\mu^T\left(\frac{du}{dy}\right)^2 - \rho\nu\epsilon + 2D_0(ck^f - k) = 0 \qquad [24]$$

and

$$\mu^{fT}\left(\frac{du}{dy}\right)^2 - \rho^f(1-\nu)\epsilon^f - 2D_0(ck^f - k) = 0. \qquad [25]$$

Using [8], and [10], and introducing the dimensionless particulate fluctuation energy and the

fluctuation energy ratio,

$$\hat{k} = \frac{k}{d^2\left(\frac{du}{dy}\right)^2}, \qquad \Omega = \frac{k^f}{k}, \tag{26}$$

[24] and [25] may be restated as

$$(C^\mu - ad\hat{k})S_0 v + (c\Omega - 1)(\hat{k})^{1/2}\frac{36v}{\left(1 - \frac{v}{v_m}\right)^{2.5v_m}\hat{\mathrm{Re}}_d} = 0 \tag{27}$$

and

$$\left(0.545\frac{\Lambda}{d} - a^f d\Omega\hat{k}\right)(1 - v) - \frac{(c\Omega - 1)}{\Omega^{1/2}}(\hat{k})^{1/2}\frac{36v}{\left(1 - \frac{v}{v_m}\right)^{2.5v_m}\hat{\mathrm{Re}}_d} = 0. \tag{28}$$

Here, the density ratio S_0 and the particle Reynolds number based on the shear rate, $\hat{\mathrm{Re}}_d$, are defined as

$$S_0 = \frac{\rho}{\rho^f}, \qquad \hat{\mathrm{Re}}_d = \frac{\rho^f d^2 \frac{du}{dy}}{\mu_0^f}. \tag{29}$$

The coefficients C^μ, $C^{f\mu}$, a, a^f, c and D_0, given by [9], [11], [14] and [15], are functions of the solid volume fraction, the physical properties of particles and scales of fluid turbulence. The effects of shear rate and particle size are reflected in $\hat{\mathrm{Re}}_d$.

When $\hat{\mathrm{Re}}_d$, the density ratio and solid volume fraction are specified, [27] and [28] form two nonlinear algebraic equations for determining the dimensionless particulate fluctuation energy and the fluctuation energy ratio. Alternatively, [24] and [25] may be solved for the particulate and fluid fluctuation energies. With $\hat{k}$ *and* Ω (or k and k^f) known, [17] and [23] provide explicit expressions for the normal and shear stresses. The predictions of the model are compared with the experimental data in the following section.

Stresses–Shear Rate Relationship

Recently, Hanes & Inman (1985) have reported a series of experiments for rapid shearing of spherical glass particles of different sizes in water and in air. They presented their results in terms of normal and shear stresses vs shear rate for fixed solid volume fractions. The experimental data of Hanes & Inman (1985) for 1.1 and 1.85 mm glass beads and water mixtures are reproduced in figures 1–6. For these glass bead diameters and the particular solid volume fractions used in the experiment, [24] and [25] are solved numerically by an iteration method. The values of k and k^f are determined for a range of shear rates between 50–270 s^{-1}. The corresponding normal and shear stresses are then computed from [17] and [23] and the results plotted as the solid lines in figures 1–6. The turbulent length macroscale is assumed to be a constant equal to 20% of the gap width and a coefficient of restitution of 0.9 for the glass bead particles is used throughout the analysis. As note by Hanes & Inman (1985), since the dimensions of the experimental apparatus used were only one order larger than the diameter of the particles, the solid volume fraction should be scaled according to

$$v = \hat{v}\frac{0.64356}{\hat{v}_m}, \tag{30}$$

where v is the effective (theoretical) solid volume fraction, $\hat{v}$ is the measured solid volume fraction in the experiment and $\hat{v}_m$ is the maximum obtainable solid volume fraction for the apparatus. The values of $\hat{v}_m = 0.55$ for 1.85 mm spheres and $\hat{v}_m = 0.64$ for 1.1 mm spheres were suggested by Hanes & Inman (1985).

Figure 1–4 show that the normal and shear stresses are rapidly increasing functions of both the solid volume fraction and shear rate. In particular, it is observed that the stresses increase in direct proportion to the square of the shear rate, as noted first by Bagnold (1954). Furthermore, they

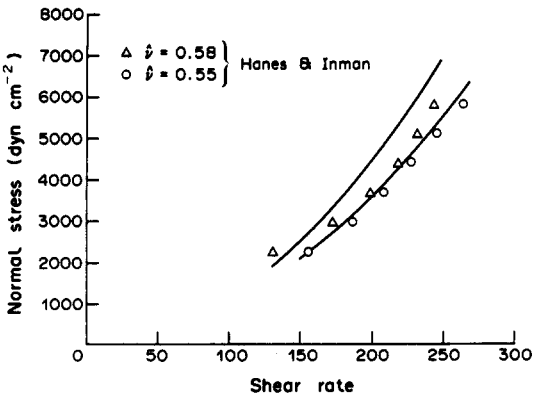

Figure 1. Variations of the total normal stresses with the shear rate for a 1.1 mm glass beads–water mixture: comparisons with the experimental data of Hanes & Inman (1985).

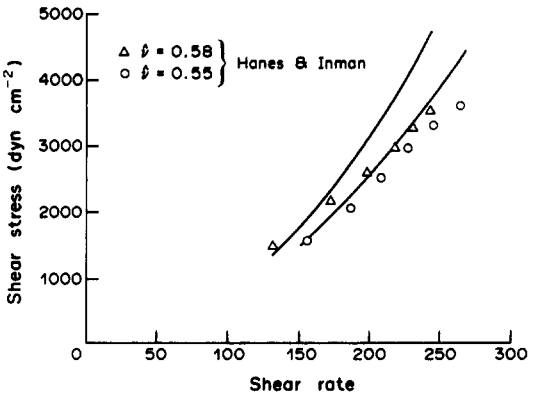

Figure 2. Variations of the total shear stresses with the shear rate for a 1.1 mm glass beads–water mixture: comparisons with the experimental data of Hanes & Inman (1985).

are rather sensitive functions of ν at these relatively high solid volume fractions ($\nu \geqslant 0.6$). From figures 3 and 4, it is noticed that an increase of 0.01 in $\hat{\nu}$ increases the stresses several fold. Figures 1–4 show that, even though some deviations are observed, the agreements between the predicted stresses and the experimental data are, generally, very good. The discrepancies observed could, in part, be due to the fact that the experimental setup used did not always produce an ideal two-phase simple shear flow. In fact, the presence of secondary flows and particle sedimentations for certain cases were reported by Hanes & Inman (1985). Furthermore, the ratio of the shear cell size to the particle diameter being of the order of 10 is rather small, which could lead to significant boundary effects and possible break down of the continuum assumption. These could, in part, be the reason for the better agreement between theory and experiment for 1.1 mm glass beads and the higher deviation for 1.85 mm glass particles observed in the figures.

Figures 5 and 6 show that the predicted stress ratios for $d = 1.1$ and 1.85 mm are in excellent agreement with the experimental data of Hanes & Inman (1985). Furthermore, these figures indicate that the stress ratios are approximately constant over the entire range of shear rate considered. This observation supports the concept of a nearly constant stress ratio for a given material, suggested by Bagnold (1954).

The particulate shear stresses as predicted by the present model for neutrally buoyant, nearly elastic particles are compared with the experimental data of Savage & McKeown (1983) for a 1.24 mm polystyrene particles–salt water mixture in figure 7. A coefficient of restitution of 0.9 for the polystyrene particles is used in the analysis. For several solid volume fractions, the predicted variations of the particulate shear stresses with shear rate are shown by the solid lines in

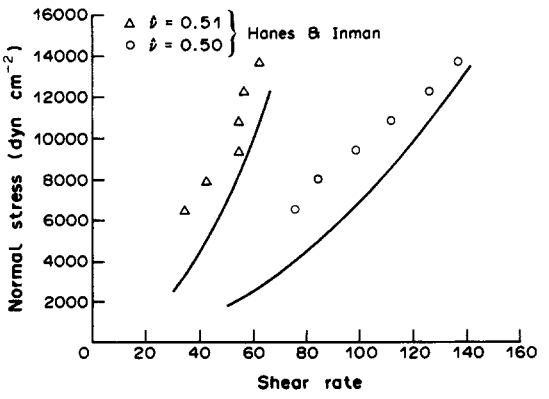

Figure 3. Variations of the total normal stresses with the shear rate for a 1.85 mm glass beads–water mixture: comparisons with the experimental data of Hanes & Inman (1985).

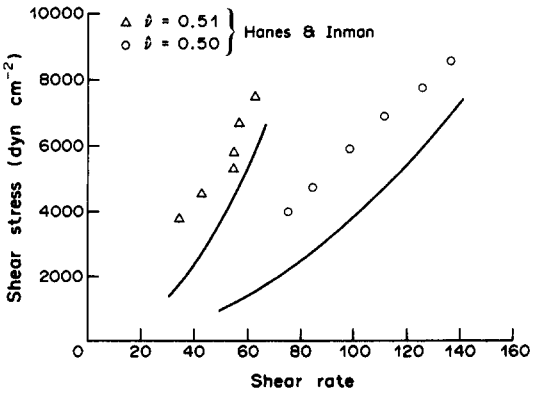

Figure 4. Variations of the total shear stresses with the shear rate for a 1.85 mm glass beads–water mixture: comparisons with the experimental data of Hanes & Inman (1985).

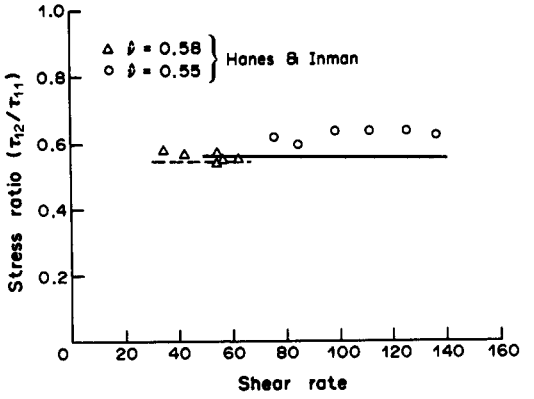

Figure 5. Variations of the stress ratios with the shear rate for a 1.1 mm glass beads–water mixture: comparisons with the experimental data of Hanes & Inman (1985).

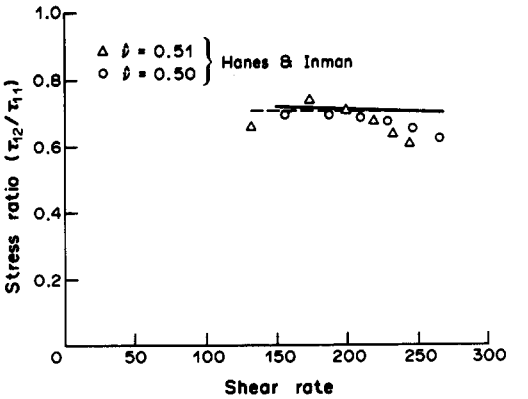

Figure 6. Variations of the stress ratios with the shear rate for a 1.85 mm glass beads–water mixture: comparisons with the experimental data of Hanes & Inman (1985).

figure 7. This figure shows that for $\nu = 0.429$ and 0.53, the predictions of the present model are in reasonable agreement with the data in both trend and magnitude. For a high solid volume fraction, $\nu = 0.57$, figure 7 shows that the experimental data is much higher than the predicted values. This discrepancy may be, in part, due to the size limitation of the experimental apparatus. Furthermore, the maximum obtainable solid volume fraction for 1.24 mm particles in the experiment was not reported. Hence, the unscaled experimental value of the solid volume fraction is used for the theoretical predictions which seems to underestimate the data for the extremely dense case.

Stress–Solid Volume Fraction Relationship

In this section, the variations of the normal and shear stresses with the solid volume fraction for simple shear flows are examined. The stresses, given by [17] and [23], may be restated as

$$|\tau_{11} + p^f| = [\tfrac{2}{3}\rho^f(1-\nu)\Omega + \gamma\rho\nu]k \qquad [31]$$

and

$$\tau_{12} = [C^\mu \rho \nu d + 0.545\rho^f(1-\nu)\Lambda\Omega^{1/2}]\left[k^{1/2}\left(\frac{du}{dy}\right)\right]. \qquad [32]$$

Nondimensionalizing [31] and [32] and using [26], we find

$$\bar{\bar{\tau}}_{11} = \frac{|\tau_{11} + p^f|}{\bar{\rho}d^2\left(\dfrac{du}{dy}\right)^2} = \frac{[\frac{2}{3}(1-\nu)\Omega + \gamma S_0 \nu]}{[(1-\nu) + \nu S_0]}\hat{k} \qquad [33]$$

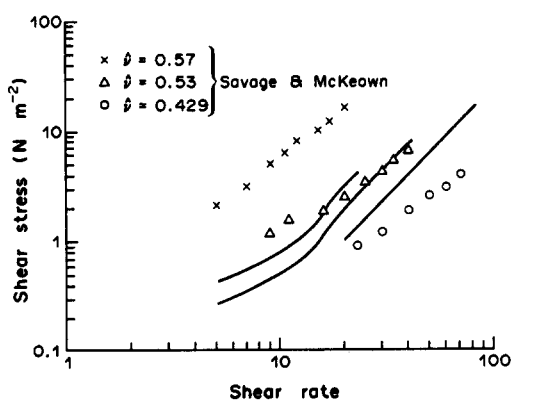

Figure 7. Variations of the shear stresses with the shear rate for 1.24 mm polystyrene beads–salt water mixture: comparisons with the experimental data of Savage & McKeown (1983).

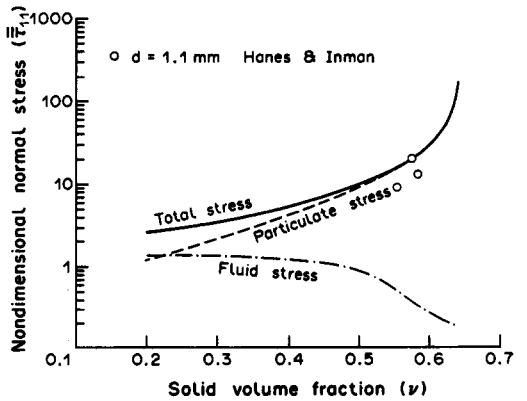

Figure 8. Variations of the nondimensional normal stresses with the solid volume fraction for glass beads–water mixture: comparisons with the experimental data of Hanes & Inman (1985).

and

$$\bar{\bar{\tau}}_{12} = \frac{\tau_{12}}{\bar{\rho} d^2 \left(\frac{du}{dy}\right)^2} = \frac{\left[C^{\mu} S_0 \nu + 0.545(1-\nu)\frac{\Lambda}{d}\Omega^{1/2}\right]}{[(1-\nu)+\nu S_0]}(\hat{k})^{1/2}, \qquad [34]$$

where $\bar{\rho}$ is the density of the mixture, given as

$$\bar{\rho} = \rho\nu + \rho^{f}(1-\nu). \qquad [35]$$

For $r = 0.9$, $\mathrm{Re}_d = 100$ and $d = 1.1$ mm, the variations of the nondimensional total normal and shear stresses with the solid volume fraction for glass bead particles in water predicted by the present model are shown in figures 8 and 9 by solid lines. The nondimensional particulate and fluid stresses are also shown in these figures by dotted lines for comparison. The experimental data of Hanes & Inman (1985) for $d = 1.1$ mm, scaled according to [30] to account for the finite size of their shear cell, are also reproduced in figures 8 and 9. These data points are obtained by averaging the data of Hanes & Inman (1985) for fixed values of $\hat{\nu}$. Note also that $\hat{\mathrm{Re}}_d$ in the experiment varied in the range 50–300. Here, however, a typical value of $\hat{\mathrm{Re}}_d = 100$ is used for the model predictions. Sensitivity analysis results (not shown here) indicate that the nondimensional stresses change only slightly when $\hat{\mathrm{Re}}_d$ varies in the range 20–2000.

From figures 8 and 9, it is observed that the total stresses predicted by the present model agree reasonably well with the experimental data. These figures show that the stresses gradually increase with the solid volume fraction up to $\nu \approx 0.6$. Beyond this value, the stresses increase rapidly with a slight increases in ν. The relative importance of particulate and fluid stresses for different solid volume fractions may be studied from figures 8 and 9. Clearly, the effect of the fluid phase is negligible for $\nu \gtrsim 0.5$. For $\nu \leqslant 0.40$, the contributions of the fluid phase to the stresses become rather significant. For very small νs, the turbulent fluid stresses become dominant. However, the analysis was not carried out for very small νs, since the algebraic expression for ϵ^f used here may no longer be satisfactory. Furthermore, it is known that an equilibrium turbulent simple shear flow for a single-phase fluid (and dilute mixture) does not exist.

At high density ratios, [35] shows that the fluid density has little effect. Therefore, it is more appropriate to use the density of particles for nondimensionalizing normal and shear stresses. Accordingly, the alternative dimensionless stresses

$$\bar{\tau}_{11} = \frac{|\tau_{11} + p^{f}|}{\rho d^2 \left(\frac{du}{dy}\right)^2}, \qquad \bar{\tau}_{12} = \frac{\tau_{12}}{\rho d^2 \left(\frac{du}{dy}\right)^2} \qquad [36]$$

are introduced. These nondimensional forms were used in most of the early works for presenting the data and theoretical predictions for granular flows. Equations [33] and [34] may now

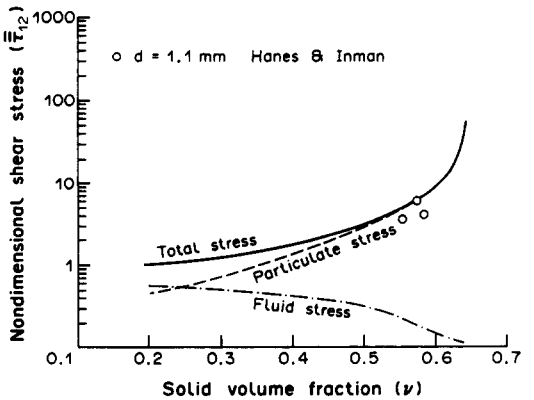

Figure 9. Variations of the nondimensional shear stresses with the solid volume fraction for glass beads–water mixtures: comparisons with the experimental data of Hanes & Inman (1985).

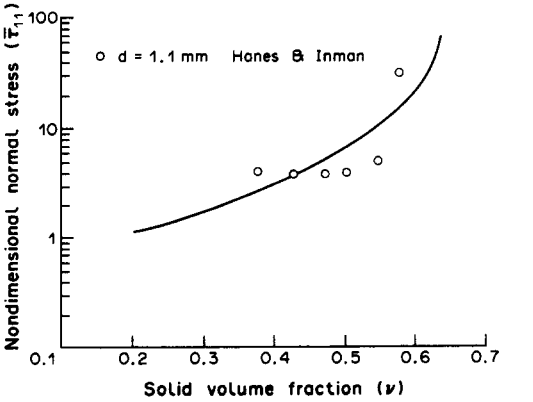

Figure 10. Variation of the normal stress with the solid volume fraction for glass beads in air ($S_0 \approx 2000$): comparisons with the experimental data of Hanes & Inman (1985).

be restated as

$$\bar{\tau}_{11} = [\tfrac{2}{3}(1-\nu)\Omega + \gamma S_0 \nu]\frac{\hat{k}}{S_0} \qquad [37]$$

and

$$\bar{\tau}_{12} = \left[C^{\mu} S_0 \nu + 0.545(1-\nu)\frac{\Lambda}{d}\Omega^{1/2}\right]\frac{(\hat{k})^{1/2}}{S_0}. \qquad [38]$$

Variations of the nondimensional normal and shear stresses with the solid volume fraction for 1.1 mm dia glass beads in air predicted by the present model, together with the experimental data of Hanes & Inman (1985), are shown in figures 10 and 11. A value of $\hat{\mathrm{Re}}_d = 100$ is used in the calculations. Although some discrepancies are observed, it appears that the predicted stresses are in reasonable agreement with the data. The relative contributions of the particulate and fluid stresses are also studied. The results (not shown here) indicate that at such a large density ratio ($S_0 \approx 2000$), the fluid stresses are two orders of magnitude lower than the particulate stresses. Therefore, the particulate stresses are essentially equal to the total stresses for the entire range of solid volume fraction studied here.

The shear stress predicted by the present model for neutrally buoyant ($S_0 = 1$), inelastic ($r = 0.2$) particles is compared with the experimental data of Bagnold (1954) for wax particles–water mixture flow in figure 12. Note that Bagnold adjusted his data to eliminate the effect of the interstitial fluid. Therefore, the presented data, presumably, represent the particulate stresses. The variation of the nondimensional total shear stress with the solid volume fraction is shown by the solid line, while the particulate and fluid stresses are shown by the dotted lines in figure 12. It is observed that the predicted particulate stresses of the present model are in good agreement with the data of Bagnold (1954) in both trend and magnitude. This figure also indicates that the fluid shear stress becomes significant for $\nu < 0.4$. Indeed, for $\nu = 0.35$ the contributions from the fluid phase become equal to that of the solid phase and for smaller values of ν the fluid shear stress becomes dominant. For high values of ν, however, the effect of the fluid phase is still negligible.

Figure 13 shows the variation of the particulate stress ratio with the solid volume fraction as predicted by the present model. The experimental data of Bagnold (1954) are also shown in this figure. It is observed that the predicted stress ratio is in a close agreement with the data for $\nu > 0.4$.

Additional results (Ma 1987) shows that both the normal and shear stresses are increasing functions of the coefficient of restitution. Furthermore, the nondimensional stresses increase gradually with the density ratio up to $S_0 \approx 20$. In addition, for moderate solid volume fractions and density ratios, the fluctuation energy density of the fluid phase is higher than that of the particulate phase. For large values of S_0 or ν, the two fluctuation energy densities become approximately equal.

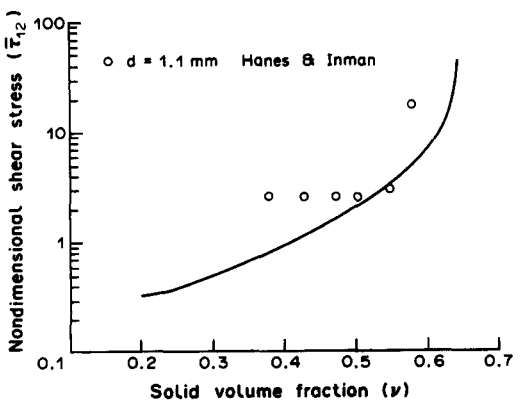

Figure 11. Variation of the shear stress with the solid volume fraction for glass beads in air ($S_0 \approx 2000$): comparisons with the experimental data of Hanes & Inman (1985).

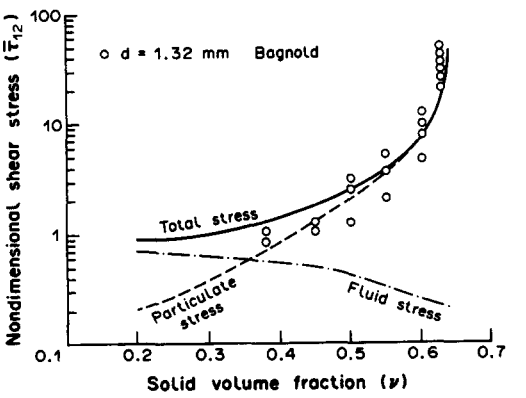

Figure 12. Variations of the shear stresses with the solid volume fraction for a neutrally buoyant particles–water mixture: comparisons with the experimental data of Bagnold (1954).

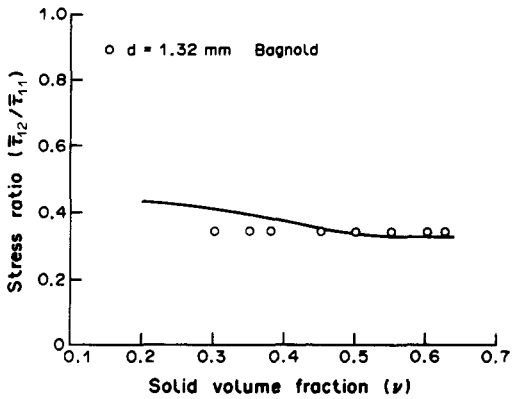

Figure 13. Variations of the stress ratios with the solid volume fraction for a neutrally buoyant particle–water mixture: comparisons with the experimental data of Bagnold (1954).

CONCLUSIONS

The turbulence model for dispersed multiphase flows developed in Part I is used to analyze the special case of relatively dense simple shear flows of solid–fluid mixtures. The system of governing equations for two-phase mixtures is simplified to a set of coupled nonlinear algebraic equations for the fluctuation energies. This system of equations is solved numerically by an iterative scheme and the normal and shear stresses for different values of the parameters are evaluated. The variations of the normal and shear stresses with the solid volume fraction, shear rate, density ratio and coefficient of restitution are studied in detail and the predicted results are compared with the available experimental data. Based on the observed favorable agreement of the theoretical predictions with the experimental data, it is concluded that the present model is capable of describing the turbulent simple shear flows of relatively dense two-phase mixtures with reasonably accuracy.

The presented results indicate that, in general, at a relatively high density ratio ($S_0 \geqslant 20$), the effects of the fluid phase on both the normal and shear stresses are negligible and the particulate stresses are dominant throughout the entire range of the nondilute solid volume fraction. For a moderate density ratio ($S_0 \leqslant 3$), however, the fluid effects become negligible only for relatively high solid volume fraction ($\nu \geqslant 0.4$) suspensions. For neutrally buoyant mixture flows, the contributions of the fluid phase to stresses become significant for $\nu \leqslant 0.4$ and the fluid stresses become dominant for $\nu \leqslant 0.3$.

The present study also shows that the normal and shear stresses for the mixtures are increasing functions of both the solid volume fraction and shear rate. In particular, they increase in direct proportion to the square of the shear rate for relatively high-speed motions. For spherical particles, the stresses increase gradually with the solid volume fraction up to $\nu \approx 0.6$. For $\nu > 0.6$, the stresses increase sharply with a slight increase in ν. The study also shows that the stress ratio, is approximately constant over the entire range of shear rate and solid volume fractions considered. This observation is in agreement with Bagnold's suggestion.

Acknowledgements—Special thanks are given to Dr D. M. Hanes for providing the details of his experimental data. This work is partially supported by NSF Grant MSM-8714687 and by the New York State Science and Technology Foundation through the Center for Advanced Material Processing (CAMP) of Clarkson University.

REFERENCES

AHMADI, G. & MA, D. N. 1986 A kinetic model for granular flows of nearly elastic particles in grain-inertia regime. *Int. J. Bulk Solid Storage Silos* **2**(3), 8–16.

AHMADI, G. & MA, D. 1990 A thermodynamic formulation for dispersed multiphase turbulent flows—I. Basic theory. *Int. J. Multiphase Flow* **16**, 323–340

AHMADI, G. & SHAHINPOOR, M. 1983 A kinetic model for rapid flow of granular materials. *Int. J. nonlinear Mech.* **19,** 177–186.

BAGNOLD, R. A. 1954 Experiments on a gravity-free dispersion of large solid spheres in a Newtonian fluid under shear. *Proc. R. Soc. Lond.* **A225,** 49–63.

BAW, P. S. H. & PESKIN, R. L. 1971 Some aspects of gas–solid suspension turbulence. *J. basic Engng* **93,** 631.

CHEN, C. P. & WOOD, P. E. 1985 Turbulence closure model for dilute gas–particle flows. *Can. J. chem. Engng* **63,** 349–360.

ELGHOBASHI, S. E. & ABOU-ARAB, T. W. 1983 A two-equation turbulence model for two-phase flows. *Phys. Fluids* **26,** 931–938.

GENCHEV, Z. D. & KARPUZOV, D. S. 1980 Effects of the motion of dust particles on turbulence transport equations. *J. Fluid Mech.* **101,** 823–842.

HANES, D. M. & INMAN, D. L. 1985 Observations of rapidly flowing granular-fluid materials. *J. Fluid Mech.* **150,** 357–380.

HETSRONI, G. 1982 *Handbook of Multiphase Systems.* Hemisphere, New York.

HETSRONI, G. & SOKOLOV, M. 1972 Distribution of mass, velocity and intensities in a two-phase turbulent jet. *J. appl. Mech.* **93,** 315.

ISHII, M. & MISHIMA, K. 1984 Two-fluid model and hydrodynamic constitutive relations. *Nucl. Engng Des.* **82,** 107–126.

JENKINS, J. T. & RICHMAN, M. W. 1985 Grad's 13-moment system for a dense gas of inelastic spheres. *Archs ration. Mech. Analysis* **87,** 355–377.

JENKINS, J. T. & RICHMAN, M. W. 1986 Boundary conditions for plane flows of identical, smooth, nearly elastic, circular disks. *J. Fluid Mech.* **171,** 53–69.

LUN, C. K. K., SAVAGE, S. B., JEFFREY, D. J. & CHEPURNIY, N. 1984 Kinetic theories for granular flow: inelastic particles in couette flow and slightly inelastic particles in a general flow-field. *J. Fluid Mech.* **140,** 223–256.

MA, D. 1987 Kinetic and turbulence models for granular and two-phase flows. Ph.D. thesis, Clarkson Univ., Potsdam, N.Y.

MA, D. & AHMADI, G. 1985 A turbulence model for rapid flows of granular materials, part II: Simple shear flows. *Powder Technol.* **44,** 269–279.

MA, D. & AHMADI, G. 1986 An equation of state for dense rigid sphere gases. *J. chem. Phys.* **84,** 3449–3450.

MA, D. & AHMADI, G. 1988 A kinetic model for rapid granular flows of nearly elastic particles including interstitial fluid effects. *Powder Technol.* **56,** 191–207.

SAVAGE, S. B. & MCKEOWN, S. 1983 Shear stresses developed during rapid shear of concentrated suspensions of large spherical particles between concentric cylinders. *J. Fluid Mech.* **127,** 453–472.

SOO, S. L. 1967 *Fluid Dynamics of Multiphase Systems.* Blaisdell, Waltham, Mass.

TAWEEL, A. M. AL. & LANDAU, J. 1977 Turbulence modulation in two-phase jets. *Int. J. Multiphase Flow* **3,** 341–351.